Artícle

Ocean wave propagation through cylindrical elements in intermediate depths

Propagación del oleaje a través de elementos cilíndricos en profundidades intermedias

CHÁVEZ-CÁRDENAS, Xavier†* & GONZÁLEZ-BRIONES, Antonio

Universidad de Guanajuato Campus Celaya-Salvatierra, Av. Javier Barros Sierra 201 Col. Ejido de Santa María del Refugio C.P. 38140 Celaya, Gto. México.

ID 1er Autor: *Xavier, Chávez-Cárdenas* / **ORC ID:** 0000-0001-6691-4380, **Researcher ID Thomson:** F-3210-2018, **CVU CONACYT ID:** 269911

ID 1er Coautor: *Antonio, González Briones* / **ORC ID:** 0000-0002-9618-5825

Abstract

The research developed has the objective of evaluating the performance of a dissipative structure formed by cylindrical elements. It has been proved that the wave interaction with circular section structures is significantly lower than the one presented with structures of different geometry, so from this point of view, the cylindrical section is not one of the first options to consider in dissipative structure elements, however, the ease of construction, the resistance of cylindrical elements to waves, the reduction in scour problems and less disturbance of the free surface, are characteristics that make cylindrical elements attractive to form a dissipative structure. The dissipative capacity of three arrays of cylindrical elements with different spacing is evaluated through the variation of the generated wave amplitude. The arrays are subjected to variations in the period and the angle of incidence of the wave. To determine the variation of the wave amplitude, simulations of the wave-structure-bottom interaction are carried out with the help of the numerical model WAPO (Wave Propagation On the coast). The results obtained are clear as to which array is the most efficient, however, due to a large number of variables it is difficult to obtain general relationships that apply to arrays other than those evaluated in this study.

Dissipation, Amplitude, Simulation

Resumen

La investigación desarrollada tiene el objetivo de evaluar el desempeño de una estructura disipativa conformada por elementos cilíndricos. Se ha comprobado que la interacción del oleaje con estructuras de sección circular es significativamente menor a la que se presenta con estructuras de distinta geometría, por lo que desde este punto de vista, la sección cilíndrica no es una de las primer opciones para considerar en elementos de estructuras disipativas, sin embargo, la facilidad de construcción, la resistencia de los elementos cilíndricos ante el oleaje, la reducción en los problemas de socavación y menores perturbación de la superficie libre, son características que hacen atractivos a los elementos cilíndricos para conformar una estructura disipativa. La capacidad de disipación de tres arreglos de elementos cilíndricos con distintas separaciones es evaluada a través de la variación de la amplitud del oleaje que se genera. Los arreglos se someten a variaciones del periodo y el ángulo de incidencia del oleaje. Para determinar la variación de la amplitud del oleaje se realizan simulaciones de la interacción oleaje-estructura-fondo con ayuda del modelo numérico WAPO (Wave Propagation On the coast). Los resultados obtenidos son claros respecto a cuál arreglo es el más eficiente, sin embargo, debido a la gran cantidad de variables es difícil obtener relaciones generales que apliquen para arreglos distintos a los evaluados en el presente estudio.

Disipación, Amplitud, Simulación

* Author's Correspondence (E-mail: x.chavez@ugto.mx)

† Researcher contributing first author

Introduction

As part of engineering, the construction of maritime structures is required to take advantage of the benefits and resources of the seas. Within the various maritime structures, protection works are essential during the construction, operation, and maintenance stages.

Specifically, in terms of shore protection, the objective of shelter or defense works is to reduce storm damage (coastal flooding and wave damage), mitigate erosion and restore ecosystems (USACE, 2002). The dissipation structure proposed in this research corresponds to coastal protection management of the *Moderation* type, according to the classification proposed by USACE (2002), which in turn is based on Pope (1997). This type of management is used for erosion mitigation and shoreline stabilization.

There are currently many prefabricated elements (PIANC-MARCOM, 2005) that are used in maritime and fluvial protection projects.

The design of maritime structures is carried out according to the stresses involved in these environments, where they must frequently operate under hostile conditions, especially waves. Goda (2010) points out that "waves are the most important phenomenon to be considered among the environmental conditions that affecting maritime structures, because they exercise the greatest influence. The presence of waves makes the design procedure for maritime structures quite different from that of structures on land" (p.3).

For the placement of large structures in the open sea or on the coasts, one of the most common ways to fix them is to support on the bottom or anchor with cables, circular section piles, which due to their geometry interact more efficiently with the waves (Avila et al., 2015). The main justification for the use of this geometry is the reduction of wave-structure interaction, which translates into lower pressures and forces on the piles, as well as a decrease in, scour problems and free surface oscillations (Govaere, 2002). The points made by Avila et al. (2015) and Govaere (2002) encourage proposing and evaluating a dissipative structure formed by cylindrical elements.

Much research has been done to understand the interaction of waves with a system of piles, where the effects on each pile are influenced by the presence of the others. From the development of an analytical method (Linton & Evans, 1990) that allows knowing with accuracy the wave modification in deep waters, to the creation of numerical models (of remarkable accuracy) that are able to simulate the wave propagation in complex coastal configurations considering the influence of the bottom on the wave (intermediate and shallow zones).

Thus, the objective of this work is to evaluate the performance of a dissipative structure formed by cylindrical elements, by estimating and comparing the wave amplitude before and after crossing the dissipative structure. The calculation of the wave amplitude is performed with the numerical model WAPO, WAve Propagation On the coast, (Silva et al., 2003 and Silva et al., 2005), the details of the model are described in the section *Numerical model*.

Among the variables evaluated, the spatial distribution of the array (separation between cylindrical elements), the wave incidence angle, and the wavelength were considered. The arrays and simulation scenarios are discussed in the *Simulations* section. Maps of wave amplitude variation are presented and described in the *Results* section, while an extensive analysis is carried out in the corresponding section.

Numerical model

Protection structures, due to their function and considering that their cost is a function of depth, are mostly located at intermediate depths, with reference to the wind-generated waves. This condition implies the influence of the bottom (seabed) on the waves, resulting in a significantly more complex phenomenon due to the wave-structure-bottom interaction. Therefore, the evaluation of wave propagation through cylindrical elements for dissipation purposes is carried out using WAPO.

The WAPO is a numerical model based on the Modified Mild-Slope Equation (MMSE) that factors in energy dissipation from both wave breaking and bottom friction and employs the second-order parabolic approximation as a lateral boundary condition to improve dispersion.

Since its derivation (Berkhoff, 1972), the Mild-Slope Equation has proven to be a very flexible and widely accepted model in coastal engineering for the simulation of wave propagation over arbitrary bathymetry in complex coastal domains. It can model the propagation of a wide spectrum of waves (short and long) allowing its use in different circumstances (Lin, 2008).

Numerically, the WAPO solves the boundary value problem arising from the elliptical form of the MMSE using the finite difference method in combination with a modified Gaussian elimination method with partial pivoting proposed by Maa et al. (1997).

Simulations

The simulations proposed to evaluate the dissipation capacity of cylindrical elements consist of analyzing variations in the separation between cylindrical elements (s) for different periods (T) and angles of wave incidence (θ).

Regarding the configuration of the cylindrical structures, three arrays are evaluated, each array consisting of three rows of cylindrical elements of 3 meters in diameter. Figure 1 shows the three arrays (I, II, and III). Array I has a separation between cylindrical elements of 4 meters (s = 4 m), in array II the separation is 9 meters (s = 9 m), and finally, s = 12 m in array III.

The bottom was established horizontally, in order not to involve more variables and to facilitate the interpretation of results. The depth (h) was set at 7.0 m so that in combination with the three wavelengths (L) associated with the periods to be evaluated (see Table 2), the intermediate water condition is guaranteed for all the simulations performed ($1/2 > h/L > 1/20$). Figure 2 shows the 3D representation of array III, which shows the detail of the flat bottom.
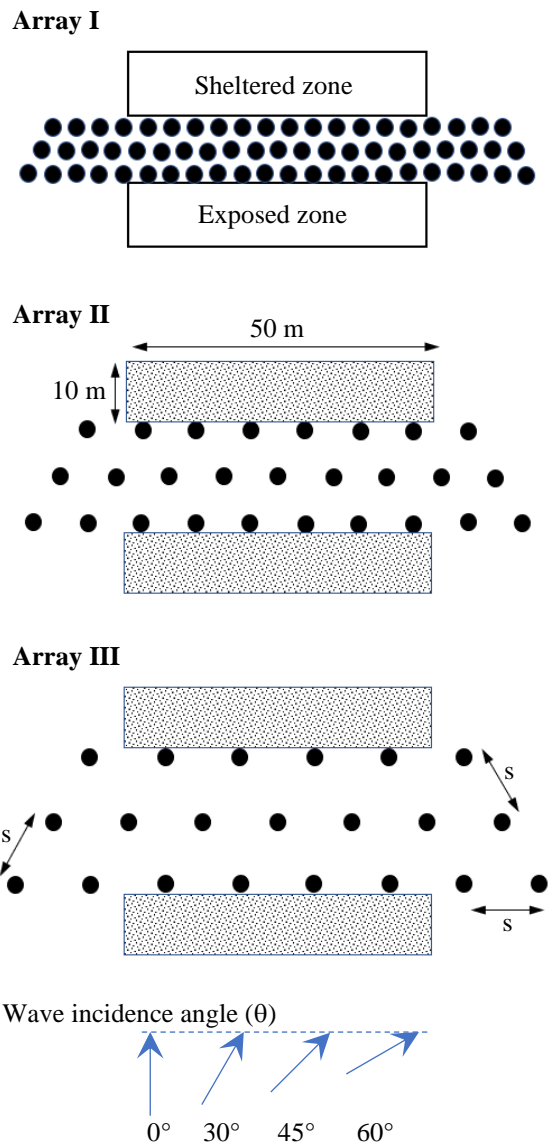

Figure 1 Arrays of the dissipative structure with their respective analysis zones (sheltered and exposed) and the representation of the wave incidence angles
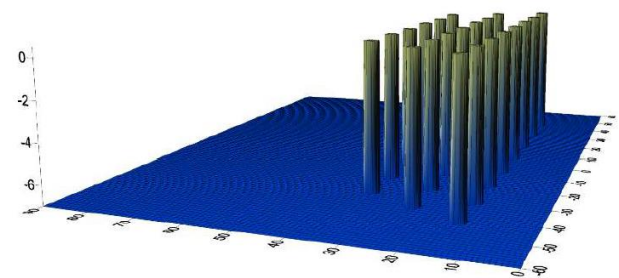

Figure 2 Array III in 3D

The dimensions that define the three proposed arrays are grouped in Table 1.

Array	Separation between elements, s (m)	Diameter (m)	Depth, h (m)
I	4	3	7
II	9	3	7
III	12	3	7

Table 1 Array dimensions

CHÁVEZ-CÁRDENAS, Xavier & GONZÁLEZ-BRIONES, Antonio. Ocean wave propagation through cylindrical elements in intermediate depths. Journal of Technological Development. 2022

The dissipation capacity of the arrays is evaluated by comparing the amplitude of the waves present in the exposed and sheltered zones. Both analysis zones correspond to a strip with a width of 10.0 m in the direction of wave propagation, measured from the edge of the stacks of the outer rows, and with a length of 50.0 m, see Figure 1.

Knowing the values of the amplitude variation before and after the interaction with the system of cylindrical elements made it possible to evaluate the protection provided by the structure in terms of transmission.

The incident wave conditions under which the simulations were performed are shown in Table 2. Both the period and the incident wave height are consistent with the actual wave conditions of the Mexican Pacific.

Period, T (s)	Wavelength, L (m)	Incident amplitude, A_i (m)	Incident angle, θ (°)
4	23.8	0.6	0
6	43.2		30
8	61.4		45
			60

Table 2 Wave conditions

The simulations were performed with the wave breaking condition of the numerical model.

Results

The combination of all the variables and values to be evaluated yields a total of 36 simulations, of which only the results of three simulations are presented in order to show and describe the amplitude maps.

The results are presented as a function of the amplitude variation defined through the dimensionless parameter A_0, which is calculated with equation 1.

$$A_0 = \frac{A_l}{A_i} \qquad (1)$$

Where:

A_0 = wave amplitude variation

A_l = local wave amplitude

A_i = incident wave amplitude

The maps cover only the area of the cylindrical elements and the respective analysis zones, exposed and sheltered zone.

Figures 3, 4, and 5 show the pattern of the variation of A_0. Each figure corresponds to a different array, but with the same incident wave: θ = 0° and T = 4 s.

In the three simulations (Figures 3, 4, and 5) the exposed zone shows an increase in amplitude ($A_0 > 1$) due to reflection upon impact with the cylindrical structures. On the other hand, the sheltered zone does show a significant change in the three arrays. In array I (Figure 3) the amplitude in the sheltered zone is notoriously decreased, $A_0 \approx 0.1$; whereas, in arrays II and III (Figures 4 and 5) the amplitude in the sheltered zone is very similar to A_i, $A_0 \approx 1$.
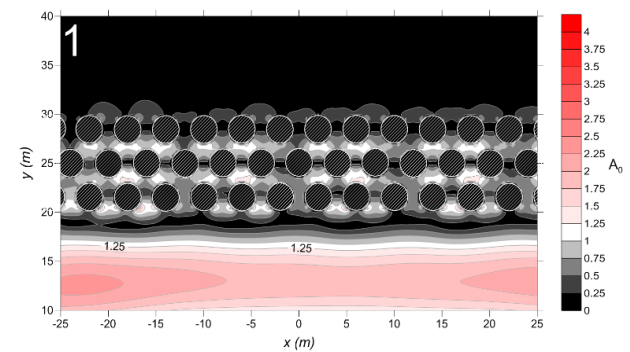

Figure 3 A_0 corresponding to the simulation of array I with θ = 0° y T = 4 s

The maximum A_0 occur next to the cylindrical structures due to the intense interaction with them. In array I a maximum A_0 of 4.25 was recorded, while in arrays II and III the maximum values were 6.25 and 5.75, respectively.
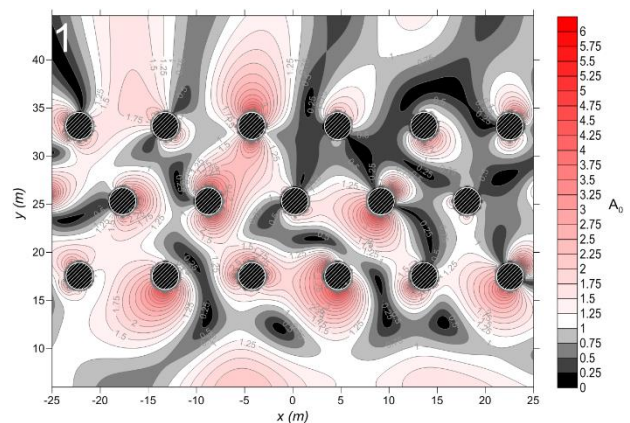

Figure 4 A_0 corresponding to the simulation of array II with θ = 0° y T = 4 s

It should be noted that the pattern of the amplitudes is not symmetrical in arrays I and II, unlike array III, this is attributed to the small asymmetry in the mesh created to represent each array, even though a small cell size, 0.15 m, was used in order to represent with acceptable accuracy the circular geometry of the structures.
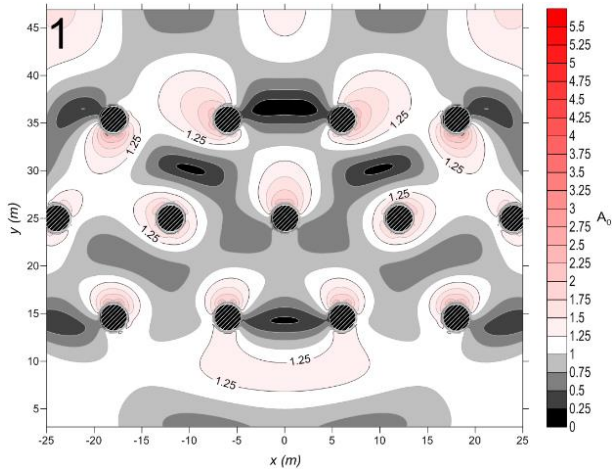

Figure 5 A_0 corresponding to the simulation of array III with $\theta = 0°$ y $T = 4$ s

Analysis

For the analysis of the 36 distribution maps of the dimensionless amplitude variation (A_0), corresponding to the 36 simulations carried out, the average values were calculated for each one of them, both in the exposed and sheltered zones. The average value before the entry of the waves into the dissipative structure, and the average value afterward, allows the evaluation of the dissipation efficiency for each simulation in terms of the amplitude transmitted through the structure.

The tables below (Tables 3, 4, and 5) clearly show the averages of A_0 in the exposed and sheltered zones for the 3 different arrays and the different simulated propagation angles. The organization of the results in this way allows a direct appreciation of the amplitude transmission effects before and after passing through the dissipative structure.

In the case of the simulations with period T=4s (Table 3), array I is the most efficient in terms of the amplitude transmitted to the sheltered zone by reducing A_i by 10%, although being such a "dense" system, its reflection levels are high, so it also generates an increase in the amplitude of the exposed zone of almost 40% for waves incident at 0° and 30°.

On the other hand, array II provides reductions in the order of 40%, except for the normal incidence wave, a scenario in which there is an increase of 5%.

Array III presented little or no efficiency when evaluating T = 4 s, as averages of $A_0 \approx 1$ were obtained in both exposed and sheltered zones.

θ (°)	Array	A_0 exposed zone	A_0 sheltered zone
0	I	1.37	0.1
	II	1.3	1.05
	III	1.05	1.03
30	I	1.37	0.13
	II	1.3	0.5
	III	1.17	1
45	I	1.07	0.12
	II	1.22	0.58
	III	1.02	1.03
60	I	0.85	0.1
	II	1	0.58
	III	0.97	0.98

Table 3 A_0 averages in the exposed and sheltered zones for T = 4 s

In the simulations for T = 6 s (Table 4), all 3 arrays show significant reductions in the amplitude recorded in the sheltered zone, however, this aspect is combined with the fact that there are increases in the exposed zone, especially for the case of array III, where its reductions in the sheltered zone are on par with its increases in the exposed zone.

θ (°)	Array	A_0 exposed zone	A_0 sheltered zone
0	I	1.18	0.07
	II	1.2	0.18
	III	1.08	0.75
30	I	1.12	0.10
	II	1.1	0.17
	III	1.20	0.85
45	I	1.00	0.13
	II	0.97	0.15
	III	1.38	0.53
60	I	0.78	0.15
	II	0.73	0.20
	III	1.37	0.45

Table 4 A_0 averages in the exposed and sheltered zones for T = 6 s

In the scenarios involving T = 8 s (Table 5), array I shows quite significant amplitude reductions even in the exposed zone, also producing almost total amplitude reductions in the sheltered zone. Array II shows increases in the averages obtained for both zones, reaching in the exposed zone increases over 40%, but keeping the sheltered zone levels below unity. Array III produces increases of up to 70% concerning A_i in the exposed zone and low reductions, including increases in the sheltered zone.

θ (°)	Array	A_0 exposed zone	A_0 sheltered zone
0	I	0.95	0.03
	II	1.42	0.58
	III	1.35	0.83
30	I	0.85	0.03
	II	1.32	0.47
	III	1.70	1.03
45	I	0.70	0.05
	II	1.07	0.35
	III	1.70	1.02
60	I	0.52	0.08
	II	0.63	0.25
	III	1.63	0.83

Table 5 A_0 averages in the exposed and sheltered zones for T = 8 s

Figure 6 shows the behavior of the average amplitude variation (A_0) in the sheltered zone for different simulated cylindrical element spacing ratios and wavelengths (s/L), the plot shows the results organized according to the incident wave propagation angle (θ).
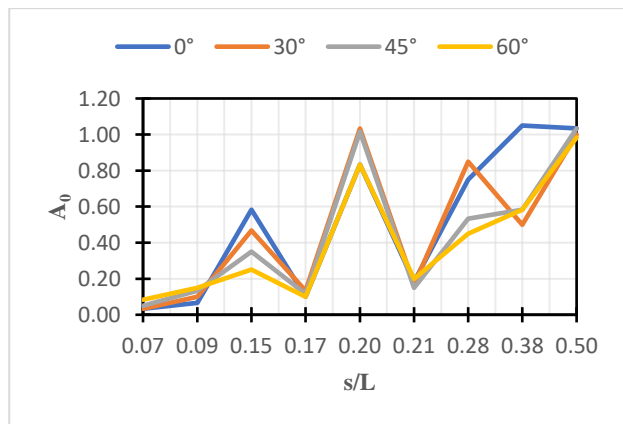

Figure 6 A_0 averages linked to the s/L ratio in the sheltered zone

It can be expressed from the above graph that the efficiency in terms of amplitude transmission tends to reduce as the s/L ratio increases, as this is close to or greater than 0.50 the protection is null and may even present amplitude magnification effects.

The A_0 recorded in the sheltered zone shows similar increasing and decreasing trends for the different angles of incidence, however, an increase in dissipation efficiency is seen as the wave propagation angle moves away from 0°.

Finally, Table 6 shows the overall averages of each array for the exposed and sheltered zones, considering all combinations of period and angle of incidence.

Having an overall average for both zones of each array allows the overall efficiency of each array to be measured.

Array	A_0 average	
	Exposed zone	Sheltered zone
I	0.98	0.09
II	1.10	0.42
II	1.30	0.86

Table 6 Overall average of A_0 by zone for each array

From Table 6 it is concluded that array III stands out due to its low level of efficiency in reducing the amplitude in the sheltered zone, combined with the fact that its placement produces an increase in amplitude in the exposed zone of about 30%.

Although array I is the one with the best numbers, showing reductions in both the sheltered and exposed zones, it is not a practical option because it is not feasible in constructive and economic terms due to the proximity of its elements, under such conditions it would be better to build a continuous breakwater.

For practical purposes, the most realistic solution for these specific conditions is array II. The disturbance caused by the system in the exposed zone reaches an average increase of only 10% against a reduction of almost 60% in the amplitude transmitted to the sheltered zone.

Conclusions

The results and analysis presented here are based on the data evaluated from the simulations performed under the conditions specified in this work. Although the results are presented here in a compact form, it is not possible to standardize them for similar configurations, where it is necessary to carefully analyze each case.

References

Ávila Armella, A., Silva Casarín, R., & Govaere Vicarioli, G. A. (2015). Evaluación de fuerzas inducidas por oleaje en sistemas de pilas cilíndricas. *Tecnología Y Ciencias Del Agua*, 19(1), 83-94. http://www.revistatyca.org.mx/ojs/index.php/tyca/article/view/1011

Berkhoff, J. C. W., (1972). Computation of combined refraction-diffraction. *in Proc. 13th Int. Conf. Coastal Engineering* (ASCE, Vancouver, Canada), Chapter 24, 471-490. https://icce-ojs-tamu.tdl.org/icce/index.php/icce/article/view/2767

Goda, Y. (2010). *Random seas and design of maritime structures. Londres*. Advanced Series on Ocean Engineering: Volume 33 (3rd Edition). World Scientific Publishing Co. Pte. Ltd. https://doi.org/10.1142/3587

Govaere, G. A. (2002). *Acción del oleaje sobre estructuras disipativas de simetría radial*. (Tesis doctoral, UNAM, D.F., México. https://repositorio.unam.mx/contenidos/92212

Lin, P. (2008). *Numerical Modeling of Water Waves* (1st ed.). CRC Press. eBook ISBN 9780429152627
https://doi.org/10.1201/9781482265910

Linton, C., & Evans, D. (1990). The interaction of waves with arrays of vertical circular cylinders. *Journal of Fluid Mechanics*, 215, 549-569.
https://doi.org/10.1017/S0022112090002750

Maa, J. P.-Y., Maa, M.-H., Li, C. & He, Q. (1997). *Using the Gaussian Elimination Method for Large Banded Matrix Equations*, Special Scientific Report, Virginia Institute of Marine Science SH 1, 48 (135). https://www.vims.edu/GreyLit/VIMS/ssr135.pdf

Pianc-Marcom (2005) Catalogue of prefabricated elements, Report of working group 36, PIANC, Brussels, Belgique. https://www.pianc.org/publications/marcom/catalogue-of-prefabricated-elements-cd-rom

Pope, J. (1997). Responding to Coastal Erosion and Flooding Damages. *Journal of Coastal Research* 13(3), 704–710. http://www.jstor.org/stable/4298666

Silva, R., Borthwick, A. G. L. & Taylor, R. E., (2005). Numerical implementation of the harmonic modified mild-slope equation, *Coast. Eng.* 52(5), 391-407. https://doi.org/10.1016/j.coastaleng.2004.12.009

Silva, R., Salles, P. & Govaere, G., (2003). Extended solution for waves travelling over a rapidly changing porous bottom, Ocean Engineering 30(4), 437-452. https://doi.org/10.1016/S0029-8018(02)00035-5

USACE (2002). *Coastal Engineering Manual* (EM 1110-2-1100, Part V, Chapter 3). US Army Corps of Engineers. https://www.publications.usace.army.mil/Portals/76/Publications/EngineerManuals/EM_1110-2-1100_Part-05.pdf?ver=g95cc9BW7REdQTCmuJzspg%3d%3d .